

and is uncorrelated from one day to the next. This gives a standard error in the trend estimate of 0.08% per decade<sup>20</sup>. An additional error is the uncertainty in determining the intersatellite biases, which are estimated from data collected during periods of satellite overlap (1–4 years). Monte Carlo simulations show that the uncertainty in specifying the intersatellite biases introduces a 0.2% per decade standard error in the trend estimate. These estimates of trend error do not include the additional uncertainty involved with questions of prediction or representation (that is, how well the 1987–1998 period represents longer-term climate change).

As a check on the error analysis, we divide the SSM/I data into two sets: local morning and local evening. For each set, completely independent derivations of the decadal trends for the three latitude zones give a maximum difference between the morning and evening trends of 0.2% per decade. This agreement indicates that diurnal effects only weakly influence the SSM/I data, in marked contrast to the significant diurnal problems affecting the MSUs. A complicated procedure is required to remove the diurnal effect from the MSU observations<sup>10</sup>, and this possibly introduces spurious trends.

The retrieval of  $W$  from SSM/I observations is less problematic than the  $T_S$  and  $T_A$  retrievals in other ways as well. The 22-GHz radiance observed by SSM/I is directly related to  $W$ , whereas the MSU measures the middle-to-upper troposphere and then infers the lower-tropospheric temperature<sup>21</sup>. Furthermore, assuming a constant  $H_{\text{rel}}$ , the 22-GHz water-vapour radiance is three times more sensitive to changes in air temperature than MSU 54-GHz radiance. For AVHRR, a continuous calibration with *in situ* data is required to remove the cooling effect of atmospheric aerosols such as those emitted by volcanic eruptions<sup>22</sup> and to correct for instrument drift and intersatellite biases<sup>2</sup>. The robustness and accuracy of the SSM/I  $W$  retrieval makes it a useful validation tool for the more complex retrievals of  $T_A$  and  $T_S$ , although we must keep in mind that they are different physical variables.

The consistency we now see emerging from various satellite observations provides new information on climate dynamics and should help resolve some of the past controversies concerning errors in the satellite data. It is notable that a relatively simple constant- $H_{\text{rel}}$  plus MALR model closely predicts the observed interannual and decadal variations of  $W$ ,  $T_S$  and  $T_A$  when zonally averaged over the tropics. Furthermore, the evidence here shows that the marine atmosphere has significantly warmed and moistened over the past decade.

Received 8 March; accepted 26 November 1999.

- Spencer, R. W. & Christy, J. R. Precise monitoring of global temperature trends from satellites. *Science* **247**, 1558–1562 (1990).
- Reynolds, R. W. & Smith, T. M. Improved global sea surface temperature analyses using optimum interpolation. *J. Clim.* **7**, 929–948 (1994).
- Wentz, F. J. A well-calibrated ocean algorithm for special sensor microwave/imager. *J. Geophys. Res.* **102**, 8703–8718 (1997).
- Hurrell, J. W. & Trenberth, K. E. Spurious trends in satellite MSU temperatures from merging different satellite records. *Nature* **386**, 164–167 (1997).
- Hurrell, J. W. & Trenberth, K. E. Difficulties in obtaining reliable temperature trends: reconciling the surface and satellite microwave sounding unit records. *J. Clim.* **11**, 945–967 (1998).
- Wentz, F. J. & Schabel, M. Effects of satellite orbital decay on MSU lower tropospheric temperature trends. *Nature* **394**, 661–664 (1998).
- Stephens, G. L. On the relationship between water vapor over the oceans and sea surface temperature. *J. Clim.* **3**, 634–645 (1990).
- Jackson, D. L. & Stephens, G. L. A study of SSM/I-derived columnar water vapor over the global oceans. *J. Clim.* **8**, 2025–2038 (1995).
- Randel, D. L. *et al.* A new global water vapor dataset. *Bull. Am. Meteorol. Soc.* **77**, 1233–1246 (1996).
- Christy, J. R., Spencer, R. W. & Lobl, E. S. Analysis of the merging procedure for the MSU daily temperature time series. *J. Clim.* **11**, 2016–2041 (1998).
- Bony, S., Duvel, J. -P. & Le Treut, H. Observed dependence of the water vapor and clear-sky greenhouse effect on sea surface temperature: comparison with climate warming experiments. *Clim. Dyn.* **11**, 307–320 (1995).
- Stone, S. H. & Carlson, J. H. Atmospheric lapse rate regimes and their parameterization. *J. Atmos. Sci.* **36**, 415–423 (1979).
- Peixoto, J. P. & Oort, A. H. *Physics of Climate* (American Institute of Physics Press, New York, 1991).
- Gaffen, D. J., Elliott, W. P. & Robock, A. Relationships between tropospheric water vapor and surface temperature as observed by radiosondes. *Geophys. Res. Lett.* **19**, 1839–1842 (1992).
- Ross, R. J. & Elliott, W. P. Tropospheric water vapor climatology and trends over north America: 1973–93. *J. Clim.* **9**, 3561–3574 (1996).

- Zhai, P. & Eskridge, R. E. Atmospheric water vapor over China. *J. Clim.* **10**, 2643–2652 (1997).
- Gutzler, D. Low-frequency ocean–atmosphere variability across the tropical western Pacific. *J. Atmos. Sci.* **53**, 2773–2785 (1996).
- Schroeder, S. R. & McGuirk, J. P. Widespread tropical atmospheric drying from 1979 to 1995. *Geophys. Res. Lett.* **25**–9, 1301–1304 (1998).
- Ross, R. J. & Gaffen, D. J. Comment on Widespread tropical atmospheric drying from 1979 to 1995, by Schroeder and McGuirk. *Geophys. Res. Lett.* **25**–23, 4357–4358 (1998).
- Wilks, D. S. *Statistical Methods in the Atmospheric Sciences* (Academic, New York, 1995).
- Spencer, R. W. & Christy, J. R. Precision and radiosonde validation of satellite gridpoint temperature anomalies. Part II: A tropospheric retrieval and trends during 1979–1990. *J. Clim.* **53**, 858–866 (1992).
- Reynolds, R. W. Impact of Mount Pinatubo aerosols on satellite-derived sea surface temperatures. *J. Clim.* **6**, 768–775 (1993).

## Acknowledgements

This work was supported by NASA as part of their pathfinder Data Set program.

Correspondence and requests for materials should be addressed to F.J.W. (e-mail: wentz@remss.com).

# The Pleistocene serpent *Wonambi* and the early evolution of snakes

John D. Scanlon\*† & Michael S. Y. Lee\*

\* Department of Zoology, University of Queensland, Brisbane QLD 4072, Australia

† Department of Biological Sciences, University of New South Wales, Sydney, NSW 2052, Australia

The Madtsoiidae were medium sized to gigantic snakes with a fossil record extending from the mid-Cretaceous to the Pleistocene, and spanning Europe, Africa, Madagascar, South America and Australia<sup>1–3</sup>. This widely distributed group survived for about 90 million years (70% of known ophidian history), and potentially provides important insights into the origin and early evolution of snakes. However, madtsoiids are known mostly from their vertebrae, and their skull morphology and phylogenetic affinities have been enigmatic. Here we report new Australian material of *Wonambi*, one of the last-surviving madtsoiids<sup>4–6</sup>, that allows the first detailed assessment of madtsoiid cranial anatomy and relationships. Despite its recent age, which could have overlapped with human history in Australia, *Wonambi* is one of the most primitive snakes known—as basal as the Cretaceous forms *Pachyrhachis*<sup>7</sup> and *Dinilysia*<sup>8</sup>. None of these three primitive snake lineages shows features associated with burrowing, nor do any of the nearest lizard relatives of snakes (varanoids). These phylogenetic conclusions contradict the widely held ‘subterranean’ theory of snake origins<sup>9–12</sup>, and instead imply that burrowing snakes (scolecophidians and anilioids) acquired their fossorial adaptations after the evolution of the snake body form and jaw apparatus in a large aquatic or (surface-active) terrestrial ancestor.

Serpentes Linnaeus, 1758  
Madtsoiidae Hoffstetter, 1961  
*Wonambi* Smith, 1976

**Revised diagnosis.** Neural spines of vertebrae high, sloping, posterodorsally, with sharp-edged anterior lamina extending to near anterior edge of zygosphenes; transverse processes extending laterally beyond zygapophyses in most trunk vertebrae, synapophyses with concave dorsal edge in lateral view; zygosphenes relatively narrow, with steep facets (20–30° from vertical); zygapophyses inclined 20° or more above horizontal; haemal keel in middle and posterior trunk region narrow and weakly defined laterally, but often distinctly bifid or trifid on the posterior third of the centrum.

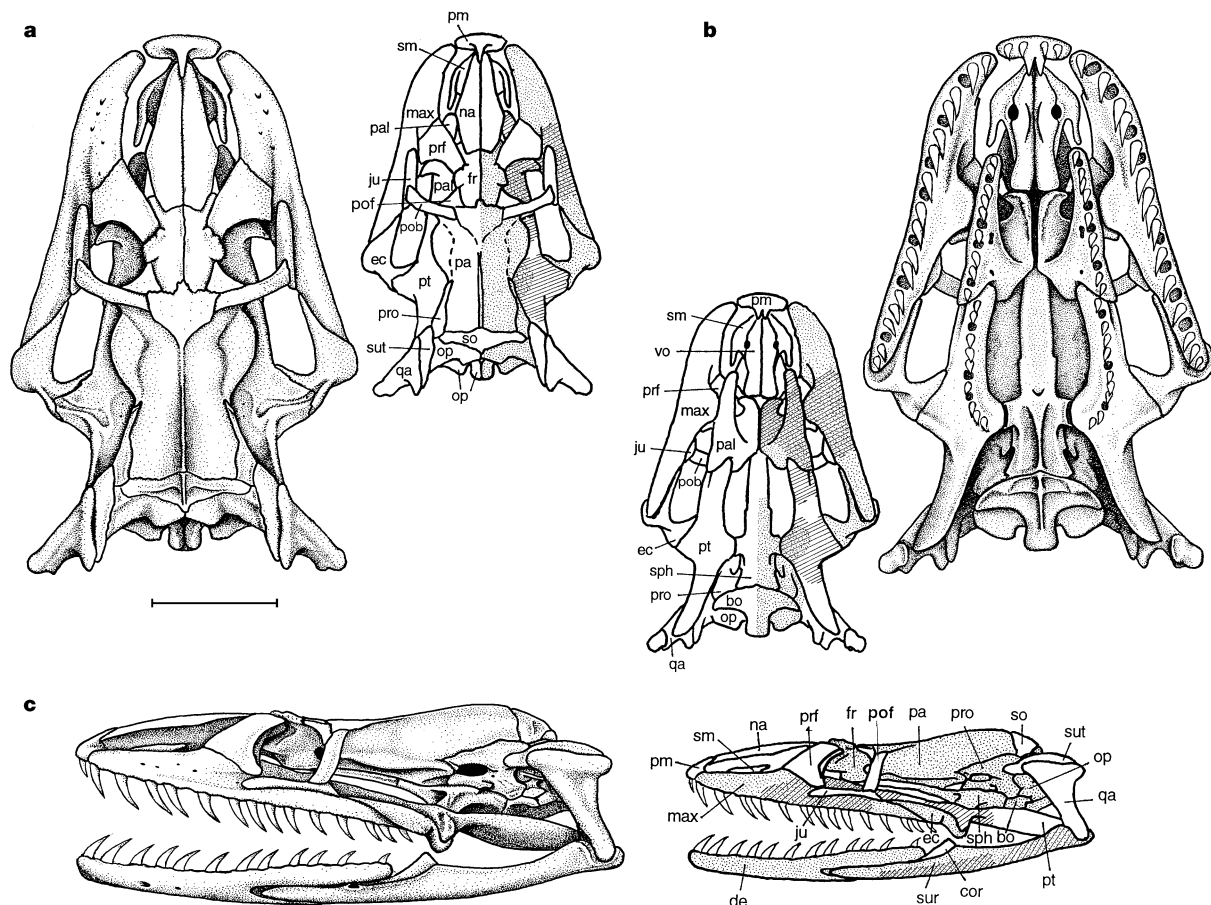


**Figure 1** Reconstruction of the skull of *Wonambi naracoortensis* Smith, 1976. **a**, Dorsal, **b**, palatal and **c**, lateral views. Small outline drawings indicate parts known in *W. naracoortensis* (stippled) and in *W. barriei* (cross-hatching). Scale bar, 30 mm (based on the largest known individual at type locality, FU1762). bo, basioccipital; ec, ectopterygoid;

cor, coronoid; de, dentary; fr, frontal; ju, jugal; max, maxilla; na, nasal; op, opisthotic; pal, palatine; pa, parietal; pm, premaxilla; prf, prefrontal; pob, postorbital; pof, postfrontal; pro, prootic; pt, pterygoid; qa, quadrate; sm, septomaxilla; so, supraoccipital; sph, sphenoid; sur, surangular; sut, supratemporal; vo, vomer.

Pterygoid tooth row near middle of bone, away from medial edge, and basipterygoid facet narrow and facing medially as much as dorsally; ectopterygoid process of pterygoid triangular in palatal view. Maxilla and dentary relatively elongate and depressed; maxilla with deep, anterolaterally directed trough on suborbital surface.

#### *Wonambi naracoortensis* Smith, 1976

**Diagnosis.** Large size (trunk vertebrae more than 20 mm and often greater than 30 mm wide, mandible length up to 160 mm, total length estimated to exceed 5 m); relatively small neural canal and deep zygosphenoid; zygapophyses inclined about 25° above horizontal; parazygantral foramina often small and multiple, weakly distinguished from pits in the same region. Palatine broad (mediolateral dimension of choanal process greater than that of tooth-bearing portion of palatine).

**Material.** Abundant vertebrae (including holotype mid-trunk vertebra, South Australian Museum P16168), ribs, and the following elements of the skull: complete maxillae, prootic, exoccipital-opisthotics, basioccipital, dentaries, compound mandibular elements; near-complete sphenoid, frontal, palatine, ectopterygoid, and parietal; and fragment of pterygoid. Most of these are represented in the partial skeletons from Henschke's Cave, Naracoorte (SAM P30178)<sup>5</sup>, but some have not been identified until this study.

**Range.** Pliocene and Pleistocene, southern Australia (Western Australia, South Australia, New South Wales)<sup>6</sup>.

#### *Wonambi barriei* Scanlon, sp. nov.

**Etymology.** Named in honour of D. John Barrie, who has collected and prepared most of the material of *W. naracoortensis*.

**Diagnosis.** Trunk vertebrae less than 15 mm wide in adults (total length estimated to be less than 3 m); relatively large neural canal and shallow zygosphenoid; zygapophyses approximately 20° above horizontal. Single, large parazygantral foramen on each side of neural arch. Palatine relatively narrow (mediolateral dimension of choanal process subequal to that of tooth-bearing portion).

**Material.** Nine well-preserved vertebrae from WW Site, Riversleigh (northwest Queensland, Australia) represent most body regions, probably from a single individual (Queensland Museum F23038, holotype mid-trunk vertebra, and F40194, paratypes). Abundant postcranial material from various other Oligo-Miocene sites at Riversleigh is referred to this taxon, including a series of cloacal and anterior caudal vertebrae from CS Site (QM F40189). Referred cranial remains include associated jaw elements from CS Site (near-complete left palatine QM F40190 and fragments of the right palatine QM F40191, right and left pterygoids QM F23047 and 23048, articular and prearticular region of left mandible QM F23077, 23078), and fragments of two maxillae from CS (QM F39932) and WW Site (QM F40193).

**Range.** Late Oligocene to Early Miocene of Riversleigh, northwest Queensland<sup>13</sup>.

**Comments.** Elements of *W. barriei* are half the linear dimensions of corresponding elements of *W. naracoortensis*, implying a roughly eightfold difference in mass. Vertebrae of *W. barriei* can be interpreted as coming from adults of a small form because of the full extent of perichondral ossification, and the proportions of the centrum and neural arch. The two species are similar in these

proportions, whereas if the smaller forms merely represented juveniles of *W. naracoortensis* they would have shorter, broader and shallower centra, and dorsoventrally thinner neural arches<sup>15</sup>. *W. barriei* exhibits narrow palatine bones, an autapomorphy not found in *W. naracoortensis* or other madtsoiids<sup>14</sup>. It also lacks the autapomorphy of *W. naracoortensis*, small and numerous parazygantral foramina. Neither of these traits appears to be correlated with size in madtsoiids or other snakes. Each species spans a considerable stratigraphic interval without noticeable change in size or morphology.

The anatomy of *Wonambi* is revised here on the basis of newly identified elements (for example, frontal and ectopterygoid of *W. naracoortensis* and pterygoid of *W. barriei*) and a re-interpretation of known elements, which have only been briefly discussed and not yet studied phylogenetically<sup>5</sup>. No other madtsoiid taxon is represented by such complete material; therefore, *Wonambi* provides the best available evidence for the phylogenetic relationships of madtsoiids with other snakes. The known elements of other madtsoiids<sup>1,3,14</sup> are similar to those of *Wonambi* and suggest that madtsoiids remained morphologically conservative throughout their long history.

The skull of *Wonambi* (Figs 1 and 2a–c) is long and low, the snout rounded, the palate very broad, and the braincase constricted behind the orbits but widening posteriorly. The parietal and frontal are most like those of *Dinilysia*<sup>8</sup> in shape (including the large lateral crests of the parietal<sup>5</sup>) and attachments to each other and surrounding bones. The snout is rigidly attached to the frontal (Fig. 1) at a vertical frontonasal suture; the frontonasal (prokinetic) joint of modern snakes is thus poorly developed (condition unknown in *Pachyrhachis*<sup>7</sup>, in *Dinilysia* the prokinetic joint is described as having only limited mobility<sup>8,16</sup>). The upper jaws have relatively tight and extensive connections to the central elements of the skull. The flat, pitted anterior end of the maxilla suggests a short ligamentous connection between the maxilla and premaxilla. The prefrontal is sutured to the maxilla but movably articulated with the frontal. There is an extensive palatine–vomere contact and small but distinct facets on the pterygoids for the basipterygoid articulations. A facet-like ‘trough’ on the suborbital region of the maxilla suggests retention of a jugal<sup>14</sup> which was also present in *Pachyrhachis*<sup>7</sup> and possibly *Dinilysia*<sup>8</sup> but lost in all extant snakes. These primitive features indicate that kinesis of the upper jaws was more limited than in modern snakes, but similar to that of

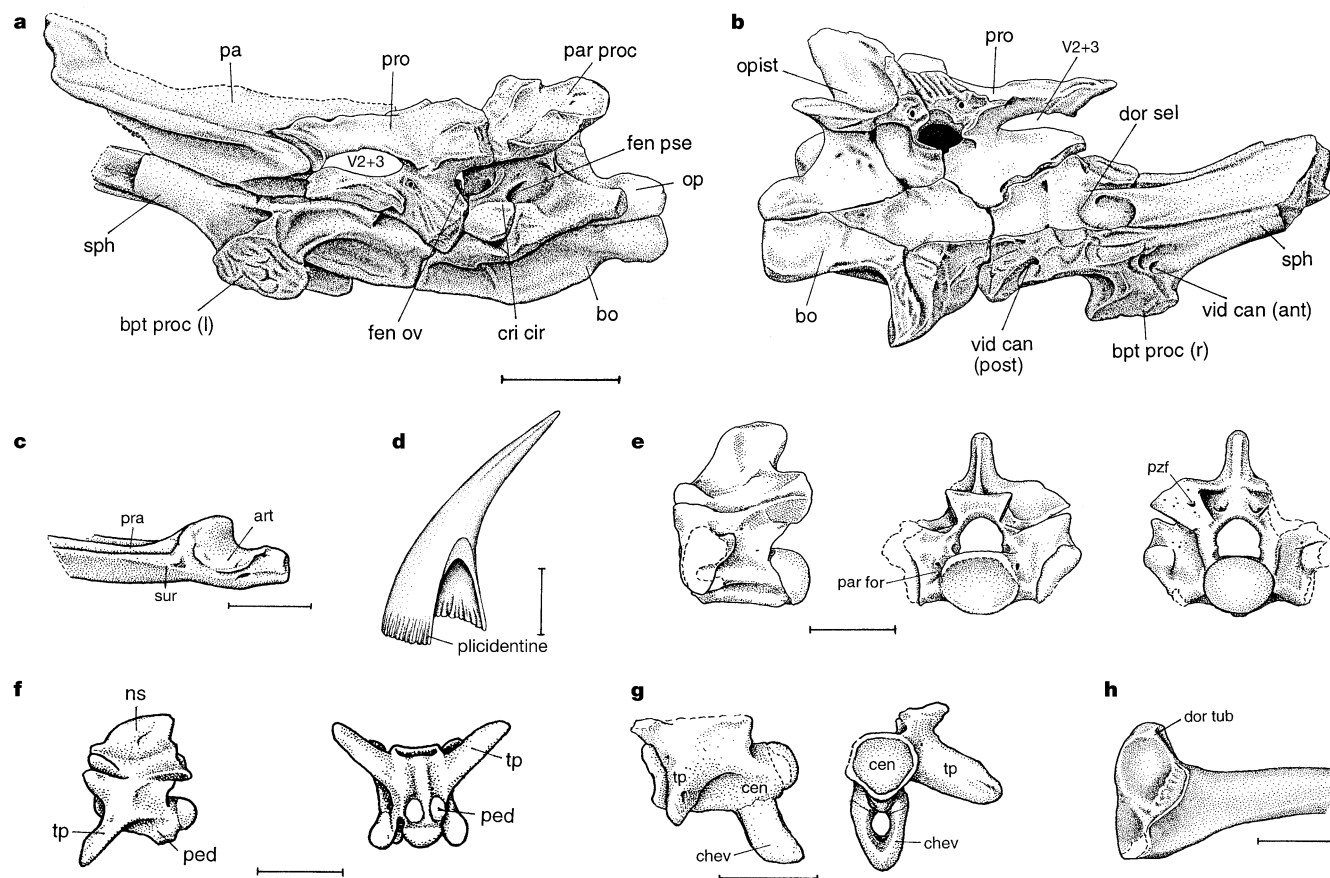


**Figure 2** Selected elements of *Wonambi* exhibiting phylogenetically important characters. **a**, External view of braincase of *Wonambi naracoortensis* (SAMP30178) in left lateral view. Scale bar, 10 mm. **b**, Internal view of braincase in right lateral and slightly dorsal view. **c**, Articular region of right mandible of *W. barriei* (QMF23077) showing sutures between articular, surangular and prearticular. Scale bar, 3 mm. **d**, Reconstructed tooth, with part of base cut away, showing plicidentine on internal and external surfaces of tooth base (based on FU1762). Scale bar, 2 mm. **e**, Holotype mid-dorsal vertebra of *W. barriei* (QMF23038) in lateral, anterior and posterior views. Scale bar, 5 mm. **f**, Caudal vertebra of *W. barriei* (QMF40189) in lateral and ventral views, showing paired pedicels near posterior end of centrum. Scale bar, 4 mm. **g**, Partial caudal vertebra of *W. naracoortensis*

(SAMP30178) in lateral and anterior views showing articulated chevron. Scale bar, 5 mm. **h**, Head of left rib of *W. naracoortensis* (SAMP30178) in anterolateral view showing dorsal tubercle. Scale bar, 10 mm. Abbreviations as in Fig. 1 plus: art, articular; bpt process (l), left basipterygoid process; bpt process (r), right basipterygoid process; cen, centrum; chev, chevron; cri cir, crista circumfenestralis; dor sel, dorsum sellae; dor tub, dorsal tubercle; fen ov, fenestra ovalis; fen pseu, fenestra pseudorotunda; ns, neural spine; par for, paracotylar foramen; par proc, paroccipital process; ped, pedicel for chevron; pra, prearticular; pzf, parazygantral foramen; top, transverse process; vid can (ant), anterior opening of vidian canal; vid can (post), posterior opening of vidian canal; V2+3, trigeminal foramen.



anilioids<sup>17</sup>. However, the mandible was longer than the skull, and the supratemporals and/or quadrates must have projected posteriorly, as in *Pachyrhachis* and macrostomatan snakes, facilitating the swallowing of large items.

The anterior trunk region, representing about one third of all trunk vertebrae, comprises relatively high and narrow vertebrae with prominent single hypapophyses, and synapophyses projecting partly below the centrum. Mid-trunk vertebrae are broader, with slightly lower and longer neural spines, more dorsally placed synapophyses, and weak, posteriorly bifid or trifid haemal keels (Fig. 2e). More posteriorly the trunk vertebrae become smaller but relatively longer. Haemal keels disappear just before the cloacal region, but reappear on the cloacals and caudals. There are at least three cloacals with fused, forked lymphapophyses. At least one anterior caudal ('pygal') lacks haemapophyses, but other caudals have paired oval facets for their attachment on the posterior part of the centrum, near the ventral midline (Fig. 2f). The haemapophyses, which remain articulated to the centrum of one caudal vertebra in *W. naracoortensis*, are fused distally into a true chevron (Fig. 2g). Trunk ribs are curved throughout their length, with their

proximal facets slightly constricted between the strongly concave diapophyseal and flatter parapophyseal surfaces, and there is a prominent dorsal process (tuber costae) adjacent to the facet (Fig. 2h). No limb or girdle elements are yet known.

Madtsoids are usually interpreted as an early appearing group of advanced snakes related to boas and pythons<sup>1,4,5,19</sup>, although it has been suggested that they might represent a much more primitive lineage<sup>2,3</sup>. Until recently, most fossil snake 'families' (including madtsoids) were not represented by sufficient cranial material for rigorous assessment of relationships<sup>1-3</sup>. The new information on *Wonambi* allows madtsoids to be included in such an analysis for the first time. Accordingly, a phylogenetic analysis was performed including all living and fossil snake families (except those known from only postcranial elements), and incorporating the most extensive set of morphological characters so far assembled for snakes (see Methods). Very similar trees resulted whether multistate characters were ordered or unordered, and whether varanoid lizards, or amphisbaenians and dibamids, were used to infer character polarity. The results (Fig. 3) show that madtsoids are among the most 'primitive' of snakes: as basal as the upper

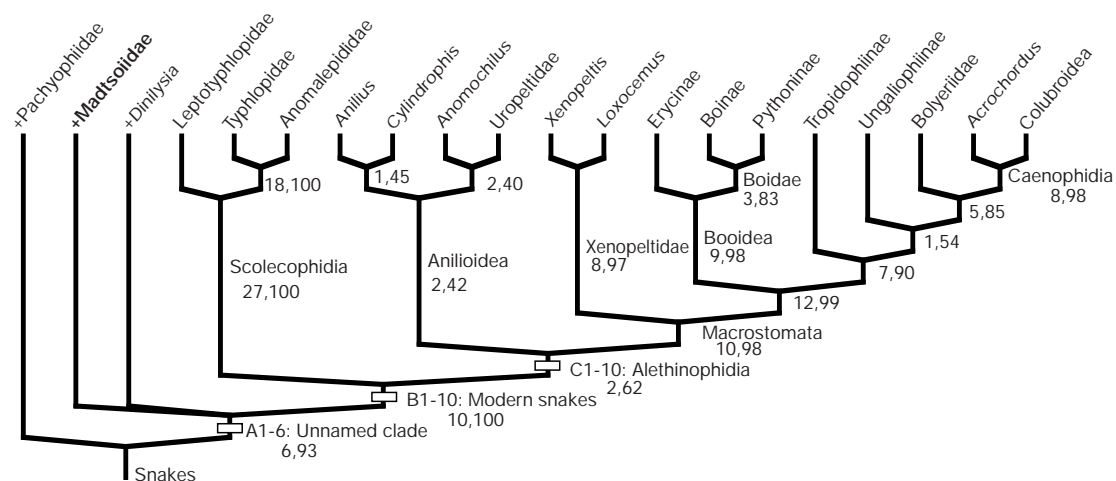


**Figure 3** Cladogram (strict consensus of two most parsimonious trees, each with length = 649, consistency index = 0.49, retention index = 0.66) showing relationships among snake lineages and the very basal position of madtsoids. This is based on a phylogenetic analysis of 234 morphological characters in 20 snake taxa (see Methods). Extinct taxa are denoted by '+'. The first number at each clade refers to Bremer support; the second refers to bootstrap frequency. Clade A, *Pachyrhachis* retains the following primitive characters shared with varanoid lizards (the derived state that unites madtsoids, *Dinilysia* and modern snakes is listed afterwards in parentheses). A1, Exoccipitals not in contact above foramen magnum (Fig. 1a) (exoccipitals in contact, excluding supraoccipital from skull margin). A2, Parietal less than 40% of skull length, that is, premaxilla–occiput dimension (Fig. 1a) (more than 40%). A3, Sagittal dimension of supraoccipital long, more than 50% transverse dimension (Fig. 1a) (short, less than 50% transverse dimension). A4, Coronoid overlaps lateral surface of surangular (Fig. 2c) (does not overlap lateral surface). A5, Free forked cloacal ribs, that is, 'lymphapophyses', absent (present). A6, Rib heads without dorsal process (Fig. 2h) (process present). In addition, *Pachyrhachis* is more primitive than all living snakes in retaining a jugal bone, tibia, fibula and tarsals, in having a distinct cervical (neck) region with short narrow ribs, and in possessing fewer than 120 precloacal vertebrae<sup>7,18</sup> (these primitive features might also characterize madtsoids and/or *Dinilysia*, but the relevant regions in both are insufficiently known). Clade B, *Pachyrhachis* (where known), madtsoids and *Dinilysia* retain the following primitive characters shared with varanoid lizards (the derived state that unites scolecophidian and alethinophidian snakes is listed afterwards in parentheses). B1, Ectopterygoid clasps dorsal and ventral surfaces of pterygoid (ectopterygoid overlaps ventral surface of pterygoid only). B2, Basipterygoid process prominent (Fig. 2) (basipterygoid processes reduced or lost; re-acquired in some booids). B3, Alar process of prootic long, narrow and distinct (Fig. 2) (alar process not distinct). B4, Crista circumfenestralis does not converge

to enclose stapedial footplate (Fig. 2a) (crista converges to partially or fully enclose stapedial footplate). B5, Paroccipital process very long (Fig. 2a) (reduced or absent). B6, Articular and surangular not fused in region of articular facet (Fig. 2c) (reduced or absent). B6, Articular and surangular not fused in region of articular facet (Fig. 2c) (articular and surangular fused). B7, Zygosphenal buttress with concave anterior edge between zygosphenes (Fig. 2e) (straight). B8, Paracotylar foramina present (Fig. 2e) (absent; reversals within Macrostromata). B9, Haemapophyses not fused to caudal centra (Fig. 2f, g) (fused to centra when present). B10, Haemapophyses are chevron-shaped, that is, joined distally (Fig. 2g) (separated distally when present). Madtsoids are more primitive than *Dinilysia* and modern snakes in retaining plicidentine on the tooth bases (Fig. 2d), and lacking prezygapophysial processes (Fig. 2e); however, conflicting characters mean that the relationships between madtsoids, *Dinilysia* and modern snakes remain unresolved. Clade C, *Pachyrhachis*, madtsoids and *Dinilysia* share with scolecophidians the following primitive (varanoid-like) characters, which are modified in alethinophidians (derived state that unites alethinophidians is listed afterwards in parentheses). C1, Medial descending lamina of frontal absent (present). C2, Frontoparietal suture straight or M-shaped (Fig. 1a) (suture U-shaped and deeply concave anteriorly). C3, Vidian canal not opening intracranially (Fig. 2a, b) (opening intracranially). C4, Laterosphenoid absent (Fig. 2a, b) (laterosphenoid present). C5, Coronoid process formed entirely by coronoid (Fig. 1c) (coronoid process formed partly or entirely by surangular). In addition, scolecophidians are more primitive than alethinophidians in several soft anatomical traits which cannot be scored in the fossil taxa. C6, Undifferentiated ventral scales (midventral scales expanded transversely). C7, Presence of first branchial arch elements (absent). C8, *Adductor mandibulae externus pars superficialis* inserts on *adductor externus medialis* (inserts on *adductor externus profundus*). C9, Single pair of thymus glands (two pairs). C10, Non-lobed kidneys (lobed).

Cretaceous *Dinilysia*<sup>8,20</sup> and only slightly more derived than the most basal known snake, the mid-Cretaceous *Pachyrhachis*<sup>7</sup>. In particular, all three fossil taxa lie outside the clade consisting of living snakes; this exclusion is supported by numerous compelling characters, a Bremer index of 10 and a bootstrap value of 100% (Fig. 3).

This analysis refutes the suggestion that *Pachyrhachis* is a derived rather than primitive snake<sup>21</sup>. Uniting *Pachyrhachis* with Macrostromata<sup>21</sup> entails a significant increase in tree length (28 steps,  $P < 0.0001$ ; see Methods) and implies reacquisition of hindlimbs and several skull bones. Other positions have also been suggested for madtsoiids (usually interpreted as booids<sup>1,4,5,19</sup>) and *Dinilysia* (as an anilioid<sup>20</sup>, booid<sup>1</sup> or basal alethinophidian<sup>12,22</sup>). All these arrangements are significantly less parsimonious than the preferred tree (all entail between 10 and 26 extra steps and can be rejected at  $P < 0.0001$ ). The arrangement obtained for living taxa is similar to those found in recent analyses<sup>1,12,22–24</sup>. There is strong support for the monophyly of booids (boas, pythons and erylins), boids (boas and pythons) and xenopeltids (*Xenopeltis* and *Loxocemus*), clades which have been either poorly corroborated or contradicted in recent studies<sup>12,22–24</sup>. There is also support for monophyly<sup>12,22</sup> rather than paraphyly<sup>23</sup> of anilioids (*Anilius*, *Cylindrophis*, uropeltids and *Anomochilus*). This region of the tree is weak<sup>12,22,23</sup>, however, as conflicting characters support nesting scoleophidians within anilioids, as the sister group of *Anomochilus*. Traits supporting this alternative arrangement, however, are almost entirely losses and reductions associated with fossoriality and miniaturization<sup>18</sup>. Within scoleophidians, a typhlopoid–anomalepidid clade<sup>12,23</sup> is strongly supported over a typhlopoid–leptotyphlopoid clade<sup>22</sup>.

The small, worm-like scoleophidians are usually thought to be the most basal snakes<sup>1,11,12,22–24</sup>, an arrangement consistent with the widely held idea that snakes evolved from tiny burrowing ancestors. This analysis indeed confirms that scoleophidians are the most basal living snakes; however, three fossil taxa emerge as even more basal than scoleophidians. Thus, the nearest relatives of snakes (mosasaurs and terrestrial varanoid lizards) and the three most basal snake lineages (*Pachyrhachis*, madtsoiids and *Dinilysia*) were all large predators with wide gapes. Mosasaurs and *Pachyrhachis* were marine, whereas madtsoiids and *Dinilysia* were either (surface-active) terrestrial or semi-aquatic<sup>1–6,14,16,25</sup>, showing none of the extensive suite of traits correlated with fossoriality<sup>17</sup>. This challenges the widespread assumption that snakes arose through a small, burrowing ancestor<sup>9–12,23</sup>: taxa straddling the lizard–snake transition are all large predators and either marine or (surface-active) terrestrial. These results suggest instead that the snake body form arose in a large, non-fossorial ancestor, perhaps for eel-like swimming<sup>26</sup> or sliding through dense vegetation<sup>27,28</sup>. Fossoriality makes its debut later in snake evolution, in ‘modern’ forms such as scoleophidians and anilioids. □

## Methods

Two-hundred and thirty-four morphological characters (191 osteological, 43 soft anatomical), adapted and expanded from recent analyses of snake phylogeny<sup>7,23,29</sup>, were scored for all snake ‘families’. Characters were polarized by reference to the nearest lizard outgroups, mosasaurs and terrestrial varanoids<sup>18</sup>, and the tree rooted with a hypothetical ancestor coded with these inferred primitive states. Use of an amphibaenian–dibamid clade as the outgroup (see ref. 18) yielded similar trees. Character descriptions and data matrix in Nexus/PAUP format are available as Supplementary Information. Analyses were performed using PAUP version 4.0 (ref. 30). Bremer support was determined using converse constraints; bootstrap values are based on 1,000 heuristic replicates. Variability within terminal taxa was treated as uncertainty (regarding the primitive state) when calculating tree lengths. Two analyses were carried out: multistate characters ordered according to morphoclines where possible, as discussed in the character descriptions; and multistate characters all unordered. The branch-and-bound search found two most parsimonious cladograms in the ‘ordered’ analysis, with madtsoiids and *Dinilysia* forming either a clade or successive sister taxa to living snakes; the strict consensus of these is shown in Fig. 3. The ‘unordered’ analysis found a single most parsimonious cladogram corresponding to the first topology. Thus, the phylogenetic results are not dependent on assumptions of character state evolution (‘ordering’). Only unambiguous characters

(those invariant under accelerated and delayed optimization) are listed in the clade diagnoses in Fig. 3. To test alternative proposed positions for each fossil taxon, the ‘backbone constraints’ command was used: the fossil taxon in question was constrained to form a clade with its putative living relatives to the exclusion of other living taxa, but other fossil taxa were allowed to ‘float’. The most parsimonious tree(s) consistent with the backbone constraint was compared with the most parsimonious (unconstrained) trees using the Templeton and Kishino–Hasegawa tests in PAUP. Tree statistics, Bremer/ bootstrap support, and Templeton/Kishino–Hasegawa test values reported (Fig. 3) are those pertaining to the ‘ordered’ analysis; those in the ‘unordered’ analysis were almost identical.

Received 1 June; accepted 16 November 1999.

1. Rage, J. C. *Handbuch der Paläoherpologie. Teil 11. Serpentes* (Gustav Fischer, Stuttgart, 1984).
2. McDowell, S. B. in *Snakes: Ecology and Evolutionary Biology* (eds Seigel, R. A., Collins, J. T. C. & Novak, S. S.) 1–50 (Macmillan, New York, 1987).
3. Rage, J. C. Fossil snakes from the Paleocene of São José de Itaboraí, Brazil. Part I. Madtsoiidae, Aniliidae. *Palaeovertebrata* **27**, 109–144 (1998).
4. Smith, M. J. Small fossil vertebrates from Victoria Cave, Naracoorte, South Australia. IV. Reptiles. *Trans. R. Soc. S. Aust.* **100**, 39–51 (1976).
5. Barrie, D. J. Skull elements and associated remains of the Pleistocene boid snake *Wonambi naracoortensis*. *Mem. Qd Mus.* **28**, 139–151 (1990).
6. Scanlon, J. D. First records from Wellington Caves, New South Wales, of the extinct madtsoiid snake *Wonambi naracoortensis* Smith, 1976. *Proc. Linn. Soc. NSW* **115**, 233–238 (1995).
7. Lee, M. S. Y. & Caldwell, M. W. Anatomy and relationships of *Pachyrhachis problematicus*, a primitive snake with hindlimbs. *Phil. Trans. R. Soc. Lond. B* **353**, 1521–1552 (1998).
8. Estes, R., Frazzetta, T. H. & Williams, E. E. Studies on the fossil snake *Dinilysia patagonica* Woodward: Part 1. Cranial morphology. *Bull. Mus. Comp. Zool. Harv.* **140**, 25–74 (1970).
9. Walls, G. L. Ophthalmological implications for the early history of snakes. *Copeia* **1940**, 1–8 (1940).
10. Bellairs, A. d’A. & Underwood, G. The origin of snakes. *Biol. Rev.* **26**, 193–237 (1951).
11. Underwood, G. *A Contribution to the Classification of Snakes* (British Museum (Natural History), London, 1967).
12. Rieppel, O. A review of the origin of snakes. *Evol. Biol.* **22**, 37–130 (1988).
13. Archer, M., Hand, S. J., Godthelp, H. & Creaser, P. in *Actes du Congrès Biochron ’97* (eds Aguilar, J.-P., Legendre, S. & Michaux, J.) 131–152 (École Pratique des Hautes Études Institute de Montpellier, Montpellier, 1997).
14. Scanlon, J. D. *Nanowana* gen. nov., small madtsoiid snakes from the Miocene of Riversleigh: sympatric species with divergently specialised dentition. *Mem. Qd Mus.* **41**, 393–412 (1997).
15. LaDuke, T. C. The fossil snakes of Pit 91, Rancho La Brea, California. *Nat. Hist. Mus. LA County Contrib. Sci.* **424**, 1–28 (1991).
16. Frazzetta, T. H. Studies on the fossil snake *Dinilysia patagonica* Woodward. II. Jaw machinery in the earliest snakes. *Forma et Functio* **3**, 205–221 (1970).
17. Cundall, D. Feeding behaviour in *Cylindrophis* and its bearing on the evolution of alethinophidian snakes. *J. Zool.* **237**, 353–376 (1995).
18. Lee, M. S. Y. Convergent evolution and character correlation in burrowing reptiles: towards a resolution of squamate phylogeny. *Biol. J. Linn. Soc.* **65**, 369–453 (1998).
19. Underwood, G. in *Morphology and Biology of Reptiles* (eds Bellairs, A. d’A. & Cox, C. B.) 151–175 (Academic, London, 1976).
20. Woodward, A. S. On some extinct reptiles from Patagonia, of the genera *Miolania*, *Dinilysia*, and *Genyodectes*. *Proc. Zool. Soc. Lond.* **1901**, 169–184 (1901).
21. Zaher, H. The phylogenetic position of *Pachyrhachis* within snakes (Squamata, Lepidosauria). *J. Vert. Paleontol.* **18**, 1–3 (1998).
22. Kluge, A. G. Boine snake phylogeny and research cycles. *Misc. Publ. Mus. Zool. Univ. Michigan* **178**, 1–58 (1991).
23. Cundall, D., Wallach, V. & Rossman, D. S. The systematic relationships of the snake genus *Anomochilus*. *Zool. J. Linn. Soc.* **109**, 275–299 (1993).
24. Heise, P. J., Maxson, L. R., Dowling, H. G. & Hedges, S. B. Higher-level snake phylogeny inferred from mitochondrial DNA sequences of 12S rRNA and 16S rRNA genes. *Mol. Biol. Evol.* **12**, 259–265 (1995).
25. Hecht, M. K. The vertebral morphology of the Cretaceous snake, *Dinilysia patagonica* Woodward. *N. Jb. Geol. Paläont. Mh.* **1982**, 523–532 (1982).
26. Nopsca, F. *Eidolosaurus* und *Pachyophis*. Zwei neue Neocom-Reptilien. *Palaeontographica* **65**, 99–154 (1923).
27. Cope, E. D. On the reptilian orders Pythonomorpha and Streptosauria. *Proc. Boston Soc. Nat. Hist.* **12**, 250–266 (1869).
28. Janensch, W. Über *Archaeophis proavus* Mass., eine Schlange aus dem Eocän des Monte Bolca. *Beitr. z. Paläont. Geol. Österreich-Ungarns* **19**, 1–33 (1906).
29. Wallach, V. & Rainer, G. Visceral anatomy of the Malaysian snake genus *Xenophidion*, including a cladistic analysis and allocation to a new family. *Amphibia-Reptilia* **19**, 385–404 (1998).
30. Swofford, D. L. *PAUP\* Version 4—Phylogenetic Analysis Using Parsimony (\*and Other Methods)*. Computer program and documentation. (Sinauer, Sunderland, Massachusetts, 1999).

Supplementary information is available on Nature’s World-Wide Web site (<http://www.nature.com>) or as paper copy from the London editorial office of Nature.

## Acknowledgements

We thank D. J. Barrie, M. Archer, R. E. Molnar, N. Pledge and R. T. Wells for access to materials, and V. Wallach, G. Underwood, J.-C. Rage, D. J. Barrie, S. E. Evans, H. W. Greene, D. Cundall, M. W. Caldwell and A. G. Kluge for discussion. This research was supported by Australian Research Council grants to M.L. and J.S. Work at Riversleigh was supported by the Australian Research Council and University of New South Wales (to M. Archer), and work at Naracoorte by Flinders University, the South Australian Museum, L. and G. Henschke, the Barrie family and numerous volunteers.

Correspondence and requests for materials should be addressed to J.S. (e-mail: jscanlon@ultra.net.au).